Nanocrystalline Cellulose: Morphological, Physical, and Mechanical Properties

Véronic Landry
Ayse Alemdar
Pierre Blanchet

Abstract

Morphological, physical, thermal, and mechanical properties of nanocrystalline cellulose (NCC) were determined. Moisture content as well as oil absorption were also studied. The NCC was obtained from sulfuric acid hydrolysis of wood pulp. Transmission electron microscopy showed that NCC has a diameter of 10 nm and a length of 150 nm. Fourier transform–Raman spectroscopy and x-ray diffraction experiments both showed that NCC has a very high degree of crystallinity. Using an Abbe refractometer, the average refractive index of the NCC in different solvents was determined to be 1.499. Hardness and elastic modulus of the homogeneous, translucent NCC films were determined by nanoindentation technique. Oil absorption and moisture content were related to the particle size.

Cellulose is the world's most abundant natural, renewable, and biodegradable polymer. It is the main constitutent in the cell walls of plants. Wood and cotton have the highest cellulose content, followed by some bast fibers, such as ramie, hemp, and flax. Cellulose is found not only in all forms of plant life but also in tunicates, a type of sea animal, and in various bacterial species.

At the molecular scale, cellulose consists of linear chains of β-D-glucopyranose units linked by (1–4) glycosidic bonds. The hyroxyl groups of the cellulose molecule tend to form intramolecular hydrogen bonds through the same cellulose molecule and intermolecular hydrogen bonds through adjacent chains (Fengel and Wegener 1984). Depending on the origin of the cellulose, the average number of glucose units in a molecule can vary from 3,000 to 10,000 (Clowes and Juniper 1968). The hydrogen bonds between cellulose molecules are arranged in a regular system resulting in a crystal-like property. On the basis of x-ray diffraction (XRD) studies and microscopic imaging, it has been shown that each crystallite region consists of at least 120 anhydroglucose units, giving a minimum chain length of 60 nm for a cellulose micelle (Ohad and Mejzler 1965). The chain widths vary according to the source of the cellulose, ranging from 3.5 nm (Côté 1964) to 5 nm (Clowes and Juniper 1968) to 10 nm (Rydholm 1965). As a consequence of its fibrous structure and strong inter- and intramoleculer hydrogen bonds, cellulose has a high tensile strength and is insoluble in most solvents.

Recently, many studies regarding the isolation and characterization of cellulose fibers, such as microfibrillated cellulose, whiskers, and nanocrystals (Favier et al. 1995a, 1995b; Dufresne et al. 1997; Dufresne and Vignon 1998; Grunert and Winter 2002; Nakagaito and Yano 2004; Alemdar and Sain 2008), have been published. The subject has received great attention by many researchers, mainly in terms of exploring the use of cellulose nanofibers in thermoplastics as a reinforcing agent. The first work on isolating cellulose whiskers and using them as reinforcement in a polymer matrix was done by Favier et al. (1995a, 1995b) at Centre de Recherches sur les Macromolecules Vegetales–Centre National de la Recherche Scientific, Grenoble, France. They demonstrated the reinforcing potential of cellulose whiskers in nanocomposites. Cellulose fibers in the form of microcrystalline cellulose have been widely used in food, cosmetics, and medical products. Because of their specific properties, they have the potential for use in optical applications like security paper, packaging, and composites. Nanocrystalline cellulose (NCC) could

The authors are, respectively, Research Scientist, Research Scientist, and Group Leader, Value-Added Wood Products and Composite Products, FPInnovations, Quebec City, Quebec, Canada (veronic.landry@fpinnovations.ca, ayse.alemdar@fpinnovations.ca, pierre.blanchet@fpinnovations.ca). This paper was received for publication in November 2010. Article no. 10-00062

Forest Prod. J. 61(2):104–112.

also be of interest to the paint and coatings industries. Cao et al. (2007) prepared water-based polyurethane films with NCC from flax. Upon the addition of NCC to 10 percent (wt/wt), they found a modulus in flexure 16 times greater than that for the polyurethane films without NCC.

The objective of the present work was to study the main properties of NCC to determine its suitability for use as a reinforcing agent in plastics, paint, and coatings. The following properties were measured: morphology (diameter and length), thermostability, hardness, reduced Young's modulus, refractive index (RI), degree of crystallinity (XRD and Fourier transform (FT)–Raman spectroscopy), oil absorption, and moisture content. Importantly, the NCC produced in this work is homogeneous and reproducible at pilot scale.

Materials and Methods

Materials

Aqueous NCC suspensions were prepared in FPInnovations' NCC pilot plant by sulfuric acid hydrolysis of a commercial bleached softwood kraft pulp according to a procedure modified from that described by Dong et al. (1998). The final pH of the NCC suspensions was approximately 2.9 and the concentration approximately 2.8 percent (wt/wt) as measured by gravimetry. The sulfur content (0.80% ± 0.05%, mean ± SD [wt/wt]) was measured by elemental analysis or by conductometric titration with sodium hydroxide. Purified linseed oil (HP-0112) used for the oil absorption tests was purchased from Laboratoire Mat, Inc. (Québec City, Quebec, Canada). Dimethyl sulfoxide (DMSO) and 4-methylmorpholine *N*-oxide (MMNO) used for the RI determination were supplied by Fisher Scientific (Toronto, Onatario, Canada) and Sigma-Aldrich (Oakville, Ontario, Canada), respectively. These solvents were used for the measurement of the RI of the NCC.

Transmission electron microscopy

The morphology of the NCC was studied using a JEOL 1230 model transmission electron microscope. A drop (5 µl) of a dilute NCC suspension (0.05%) was deposited on the carbon-coated grids and allowed to dry at room temperature. Working voltage of the system was 80 kV. The length distribution of the NCC was calculated using the METAMORPH software.

X-ray diffraction

Diffractogram of the NCC was obtained from a x-ray diffractometer (Siemens/Bruker). The source used was a graphite monochromatized copper radiation (K$\alpha = 1.5458$ Å). The instrument consisted of a Kristalloflez 760 generator, a three-circle goniometer, and a Hi-Star area detector equipped with GADDS software. The operation power was 40 K and 20 mA. NCC was placed in thin-walled (thickness, 0.01 mm), glass capillary tubes (diameter, 1.0 mm). To determine the cellulose crystal size, the Scherrer equation was used (Oh et al. 2005):

$$T = \frac{0.94\lambda}{B_{1/2}\cos\theta} \quad (1)$$

where T is the crystal size, λ is the x-ray wavelength, $B_{1/2}$ is the diffraction line-width at half-peak size, and θ the Bragg angle. XRD was also used to measure the degree of crystallinity of the NCC according to the following equation:

$$C\,(\%) = \frac{I_c}{I_{total}} \times 100 \quad (2)$$

where I_c is the area under the profile of the peaks only, I_b is the area of the profile of the background only with correction for air scattering, and I_{total} is the total intensity ($I_c + I_b$; Alemdar and Sain 2008). To separate the amorphous and crystalline phases from the air scatter, two diffractograms were taken: one with the sample and one without the sample. The latter was subtracted from the sample's diffractogram using the GADDS software. The remaining data were analyzed using a two-dimensional background estimation algorithm to remove the sharp crystalline contributions (I_b). Then, to obtain the crystalline part (I_c), the program subtracted the amorphous surface of the total intensity (I_{total}).

FT-Raman spectroscopy

FT-Raman spectra of the NCC was recorded using a MultiRam spectrophotometer from Bruker Optics (Billerica, Massachusetts). The Raman system is equipped with a 1,064-nm, 1,000-mW, continuous-wave diode-pumped neodymium:yttrium-aluminum-garnet laser. The NCC was pressed into pellets, and the FT-Raman spectra of the NCC was recorded at a laser power of 300 mW at a precision of 1 cm^{-1}. In total, 300 scans were taken. The OPUS software was used to find peak positions. Crystallinity was estimated according to the univariate method described by Agarwal et al. (2010). The following correlation equation was used for this purpose:

$$X_{Raman} = \frac{(I_{380}/I_{1,096}) - 0.0286}{0.0065} \quad (3)$$

Thermogravimetric analysis

Thermogravimetric analysis was performed to study the thermal stability of the NCC. Experiments were performed using a thermogravimetric analyzer (Model TGA/SDTA 851^e; Mettler-Toledo) with a heating rate of 10°C/min under a nitrogen atmosphere.

Refractive index

An extrapolation technique described by Saveyn et al. (2002) was used to determine the RI of the NCC. The freeze-dried NCC was dispersed in three solvents—distilled (DI) water, DMSO, and MMNO—at seven different concentrations ranging from 0.1 to 1 percent (vol/vol). The RI of the NCC in different solvents was measured using an Abbe Refractometer A300A (LR45302; Fisher), providing RI values to an accuracy of four decimal places. The RI recorded for known solute concentrations was extrapolated to 100 percent concentration to calculate the bulk RI of the NCC. Validation of the RI values obtained using the Saveyn et al. method was performed using an ellipsometer.

Hardness

Nanohardness (H) and the reduced Young's modulus (E_r) values of the NCC films were determined by depth-sensing indentation using the TI 900 Nano-triboindenter instrument (Hysitron, Inc.) equipped with a Berkovich pyramidal indenter in agreement with the ISO 14577-4 Standard.

Homogeneous, translucent films of the NCC were prepared on glass substrate from water solution by solution casting. The test procedure involves continuous monitoring of the load and the indenter's position during the loading and unloading cycles. An example of a load-displacement (*F*-*h*) curve is shown in Figure 1.

The initial slope of the unloading curve at the maximum load is defined as the stiffness (*S*) of the material, which together with an experimentally derived tip area function is used to calculate nanohardness and reduced Young's modulus by the following equations:

$$H = \frac{F_{\max}}{A} \tag{4}$$

$$E_r = \frac{1}{2}\frac{dF}{dh}\left(\frac{\pi}{A}\right)^{1/2} \tag{5}$$

where F_{max} is the maximum applied load, A is the surface area function, and dF/dh is the stiffness at the maximum load. In such case, E_r represents the reduced Young's modulus:

$$\frac{1}{E_r} = \frac{1-\upsilon\upsilon'}{E'} + \frac{1-\upsilon\upsilon_i}{E_i}$$

where E' and E_i are the elastic moduli of the NCC film and the indenter, respectively, and $\upsilon\upsilon'$ and $\upsilon\upsilon_i$ are the Poisson's ratios of the film and the indenter, respectively. For a diamond indenter, $E_i = 1{,}140$ GPa and $\upsilon\upsilon_i = 0.07$.

Sample hardness and reduced Young's modulus were analyzed by normalizing the penetration depth (hc) and the contact depth (*a*; Fig. 2). The sample thickness (tc) was measured by ellipsometry and found to be 1,600 nm. The load range was from 20 to 2,000 μN, and load cycle was on the order of 5 seconds loading, 2 seconds holding, and 5 seconds unloading.

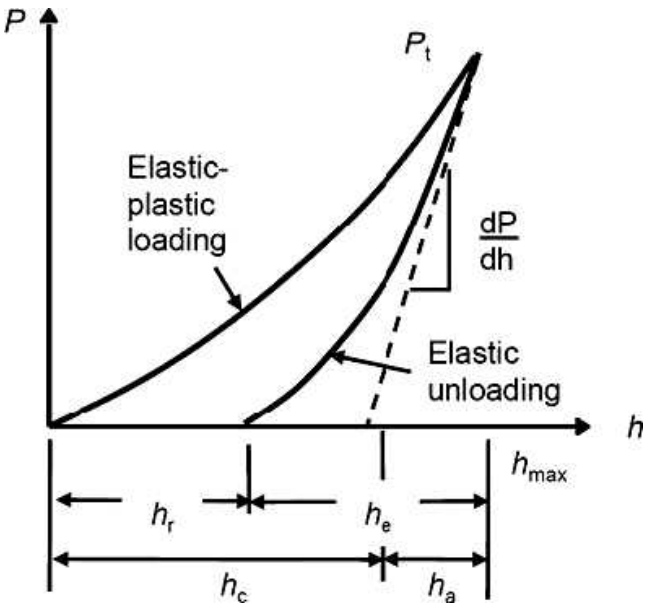

Figure 1.—Typical load-displacement curve obtained by depth-sensing indentation. h_r *= residual depth;* h_c *= contact depth;* h_e *= elastic recovery depth;* h_a *= sink-in depth;* h_{max} *= total depth.*

NCC grinding

Because NCC is hydrophilic, it is difficult to obtain a good dispersion of NCC fibers at the nanoscale in hydrophobic polymers, such as poly(methyl) methacrylate (PMMA) or polyolefins (polystyrene, polyethylene, and polypropylene). However, hydrophilic materials can still be used in hydrophobic polymers. For instance, alumina and silica are added in different hydrophobic polymers (e.g., PMMA) to improve mechanical properties. In this case, the size of the particles is very important, because no further dispersion will occur as a result of the low compatibility with the polymer matrix. NCC freeze-drying leads to the formation of large platelets of low density. To study how the NCC would perform at different particle sizes in hydrophobic polymers, three powders were prepared from the freeze-dried NCC platelets. A jar mill was used to prepare the finer particles. Jar mill treatment was performed for 48 hours. Two powders were prepared by using a laboratory mill (Model 4; Thomas Scientific). Two grids were used, the first with an aperture of 0.5 mm and the second with an aperture of 1.0 mm. The powder obtained from the jar mill treatment led to a mean particle size of 4 μm as determined by optical microscopy.

Oil absorption

The oil absorption of the NCC particles was studied in accordance with American Society for Testing and Materials Standard D281-95 (ASTM 1995). One gram of the NCC was placed upon a glass plate. Raw linseed oil was added drop by drop to the NCC powder. After each addition, the oil was thoroughly incorporated in the NCC powder by spatula rub-out. The weight of linseed oil that must be taken up by a given weight of NCC is defined as the oil absorption value. Because this value is closely related to the particle size, the latter was determined for the NCC powders of three different sizes.

Moisture content

The moisture content of the NCC was measured. The three NCC powders were placed at 20°C and 50 percent relative humidity for 48 hours. Then, samples were weighed and placed in an oven at 105°C for 48 hours, after which they were weighed second time.

Results and Discussion

Transmission electron microscopy

Figure 3 shows the TEM images of the NCC taken at different magnification levels. It is clear from these images that the length of the cellulose nanocrystals is approximately 100 to 200 nm, with a diameter of 10 nm. The length of the NCC was measured using the METAMORPH software. The length distribution of the NCC was calculated, and the mean length was 110 nm. There have been several published studies on the extraction of cellulose nanofibers from different resources, such as wheat straw (Bhatnagar and Sain 2005, Alemdar and Sain 2008), tunicin (Favier et al. 1995a), wood (Beck-Candanedo et al. 2005), and banana (Deepa et al. 2010). The width and length of these nanofibers ranged from 10 to 200 nm and from 100 nm to several micrometers, respectively, depending on the resource and the extraction method used. In comparison, the length of the NCC prepared in the present study is similar. The aspect ratio (length/diameter) of the fillers as well as

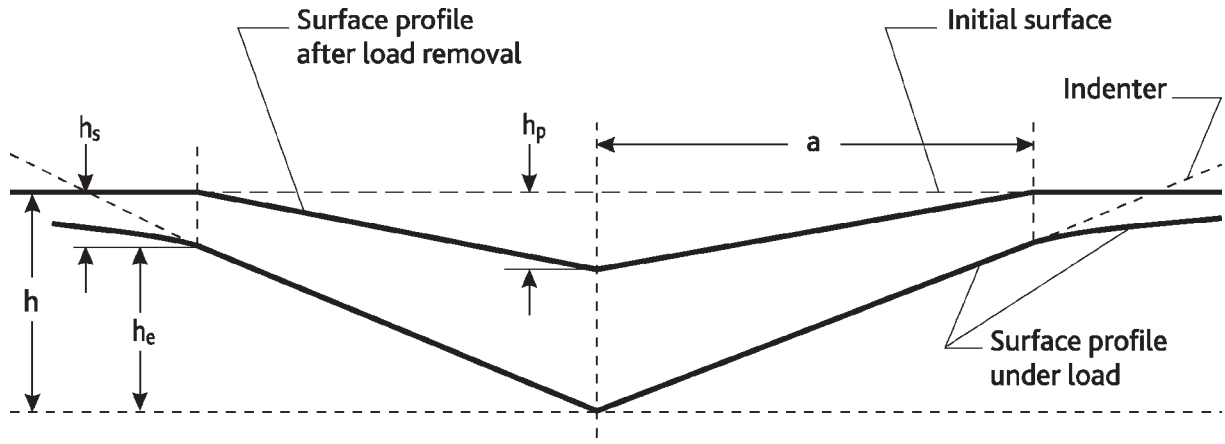

Figure 2.—Parameters of surface deformation under nanoindentation. h = *total depth during loading;* h_s = *depth below the initial surface where the indenter is not in contact with the material;* h_p = *residual depth after complete unloading;* a = *radius of contact between the indenter and the surface;* h_e = *elastic recovery depth.*

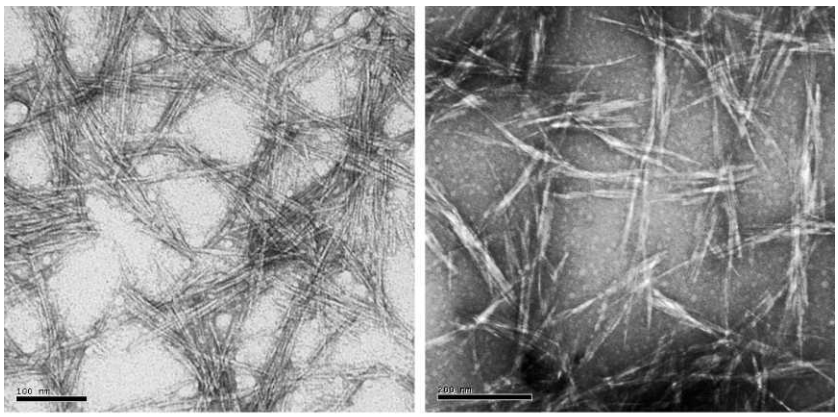

Figure 3.—Transmission electron microscopy images of the nanocrystalline cellulose: original magnifications ×150,000 (a) and ×100,000 (b).

their length are also important parameters that define the reinforcement capacity of the fillers in polymers—the higher the aspect ratio, the higher the reinforcement capacity. In addition, having cellulose fibers in nanosize increases the surface area of the fillers, which have a larger contact area with the polymers.

X-ray diffraction

The XRD pattern of the NCC is presented at the Figure 4. In the past, XRD experiments were used to study the degree of crystallinity of many materials, including cellulose I (native cellulose). Three peaks can be observed on the diffratogram of the NCC shown in Figure 4: the first at 15.5°, the second at 22.7°, and the last (smaller than the first two) at 35°. These three peaks are characteristic of the cellulose I (Chen and Yokochi 2000, Borysiak and Doczekalska 2005, Oh et al. 2005, Rosa et al. 2010). The peaks at 22.7° and 15.5° represent the I_{beta} (or β) and the superposition of the reflections 1 to 10 and 110 of the cellulose I crystal lattice, respectively. Sharp peaks were obtained, which means that the size of the crystallites is high. The presence of amorphous chains leads to broad peak (amorphous halo) situated at approximately 21° in 2θ (Fink et al. 1987, Nishiyama et al. 2002). During acid hydrolysis, amorphous cellulose is removed, which leads to a highly crystalline product. For cellulose samples and many other materials, an important degree of crystallinity or structure often leads to better mechanical properties.

Cellulose crystallite size was measured using the Scherrer equation. The crystallite size was 3.5 ± 0.1 nm. These results are similar to those found by Chen and Yokochi (2000) for cotton. The cotton cellulose crystallite size those authors determined varied from 3.9 and 6.7 nm, depending on the sample, with an average of approximately 5.2 nm. Hamad and Hu (2010) showed that crystallite size varies according to the acid hydrolysis conditions. Those authors found crystallite sizes of between 5.9 and 16.8 nm. The crystallite size determined reveals that the NCC in our study is polycrystalline, because the TEM experiments have shown that the length of the cellulose nanocrystals is approximately 100 to 200 nm, with a diameter of 10 nm.

Cellulose crystallinity was also measured by XRD according to Equation 2 and found to be 78 ± 3 percent. Different values were found in the literature for NCC, and those results have shown that the crystallinity varies importantly according to methods of preparation and

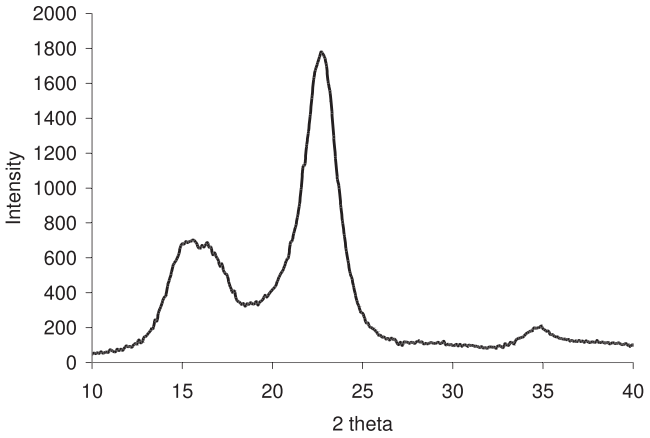

Figure 4.—Diffractogram of the nanocrystalline cellulose.

determination of crystallinity. Agarwal et al. (2010) found crystallinity of 91.0 and 67.3 percent for NCC. Hamad and Hu (2010) found crystallinities of NCC prepared from the acid sulfuric hydrolysis process of between 58.6 and 89.1 percent. Hydrolysis conditions (i.e., temperature, sulfuric acid concentration, and treatment time) were found to change the crystallinity of the NCC significantly.

FT-Raman spectroscopy

FT-Raman spectroscopy was used to study the structure of NCC as well as the degree of crystallinity. FT-Raman spectroscopy presents major advantages over FT-infrared spectroscopy for the analysis of biological samples. Water shows only weak bands in Raman spectroscopy, which helps reduce the background of the spectra (Wiley and Atalla 1987). The low-frequency region is difficult to observe in infrared spectroscopy, which is not the case in FT-Raman spectroscopy. Therefore, FT-Raman spectra are easier to interpret than infrared spectra for biological materials such as wood components. The NCC spectrum is presented at Figure 5 and can be separated into several regions. The low-frequency region from 250 to 550 cm^{-1} presents several small bands that are closely spaced. Most of these bands can be attributed to the skeletal-bending modes of the CCC, COC, OCC, and OCO internal coordinates (Wiley and Atalla 1987). Agarwal et al. (2009) developed a method to measure the crystallinity of cellulose I samples using FT-Raman spectroscopy. One of the bands those authors found is at approximately 380 cm^{-1}. They noticed that the intensity and bandwidth of this band are closely related to the degree of crystallinity, and they showed that the higher and sharper this band, the higher the degree of crystallinity. In the FT-Raman spectrum of the NCC, a sharp band can easily be seen at 378 cm^{-1}, which means that the degree of crystallinity of this sample is high. This band is also characteristic of cellulose I (Schenzel et al. 2008). According to the study by Agarwal et al. (2009), for high-crystallinity cellulose samples, bands around 437 and 458 cm^{-1} should also be easily identifiable. That is the case for the FT-Raman spectra of the NCC; bands at 457 and 436 cm^{-1} were observed. For low-crystallinity samples, these two bands merge into one broad band.

The region from 550 to 950 cm^{-1} presents few bands of low intensity. The band at 896 cm^{-1} is more intense. The presence of this band is related to the HCC and HCO bending at C-6. According to Wiley and Atalla (1987), the intensity of this band is proportional to the amount of disorder in the cellulose sample. The band found in the FT-Raman spectrum of the NCC is small and sharp compared to those found in cellulose from Valonia and ramie fibers. In the preparation process of the NCC, amorphous cellulose is removed, which explains the presence of a sharp peak on this spectra (Proniewicz et al. 2001). The appearance of a shoulder at the higher frequency of this band may indicate the existence of two nonequivalent C-O-C bonds, which does not seems to be the case here.

The region from 950 to 1,180 cm^{-1} represents mostly CC and CO streching motions. For high-crystallinity cellulose samples, a band at approximately 1,096 and 1,120 cm^{-1} can be seen (Agarwal et al. 2009). For cellulose samples, which present an important proportion of amorphous cellulose, these bands merge and form one broad band. Our study shows one more time that the degree of crystallinity of the NCC is quite high, because one peak at 1,095 and one peak at 1,119 cm^{-1} were observed. The region from 1,180 to 1,500 cm^{-1} presents few medium-intensity bands that represent HCC, HCO, HCH, and HOC bending modes. The region that goes from 2,800 to 3,000 cm^{-1} represents the CH and CH_2 streching modes of the cellulose molecule.

Crystallinity was measured according to the univariate method (Agarwal et al. 2010) and was found to be 74 percent. This result is close to that found by XRD (78%), especially if compared with the results found by Agarwal et al. (2010), who reported that the difference between the XRD and FT-Raman results is far more important.

Thermogravimetric analysis

Thermal stability of cellulose nanocrystals is important, especially for thermoplastics applications, because the processing temperature often exceeds 200°C (Wang and Huang 2007). For this reason, thermal stability of the NCC was studied. Results are presented in Figure 6, and as can be seen, the weight-loss curve of the NCC has several sections. From 30°C to approximately 120°C, the weight loss is associated with the evaporation of the water molecules contained in the samples. Then, a plateau appears until 290°C. Cellulose usually undergoes degradation at temperatures ranging from 250°C to 400°C (Randriamanantena et al. 2009). Amorphous polymer chains undergo degradation before cellulose crystals (starting from 250°C), and the temperature range associated with the degradation of the cellulose is related to the purity of this semicrystalline polymer. XRD and FT-Raman experiments have shown that the NCC used here contains approximately 25 percent amorphous cellulose, which explains the degradation between 200°C and 300°C. The NCC is nearly decomposed completely into volatile products, such as CO_2, at 400°C. The degradation of the NCC was found to start only at 290°C, which can be explained by two reasons. The first is the absence of amorphous chains. Highly structured nanocellulose crystals present higher-temperature degradation. The second is that the hydrogen ions (H^+) from acid hydrolysis were replaced by alkaline ions (Na^+). Sulfuric acid is a well-known dehydration catalyst, which means that weight loss occurs at lower temperature when hydrogen ions are present. When alkaline ions replaced hydrogen ions, the dehydration catalyzed by acid is inhibited. The sharp weight loss starting at 290°C and lasting until 320°C can be associated with two different degradation processes (Arsen-

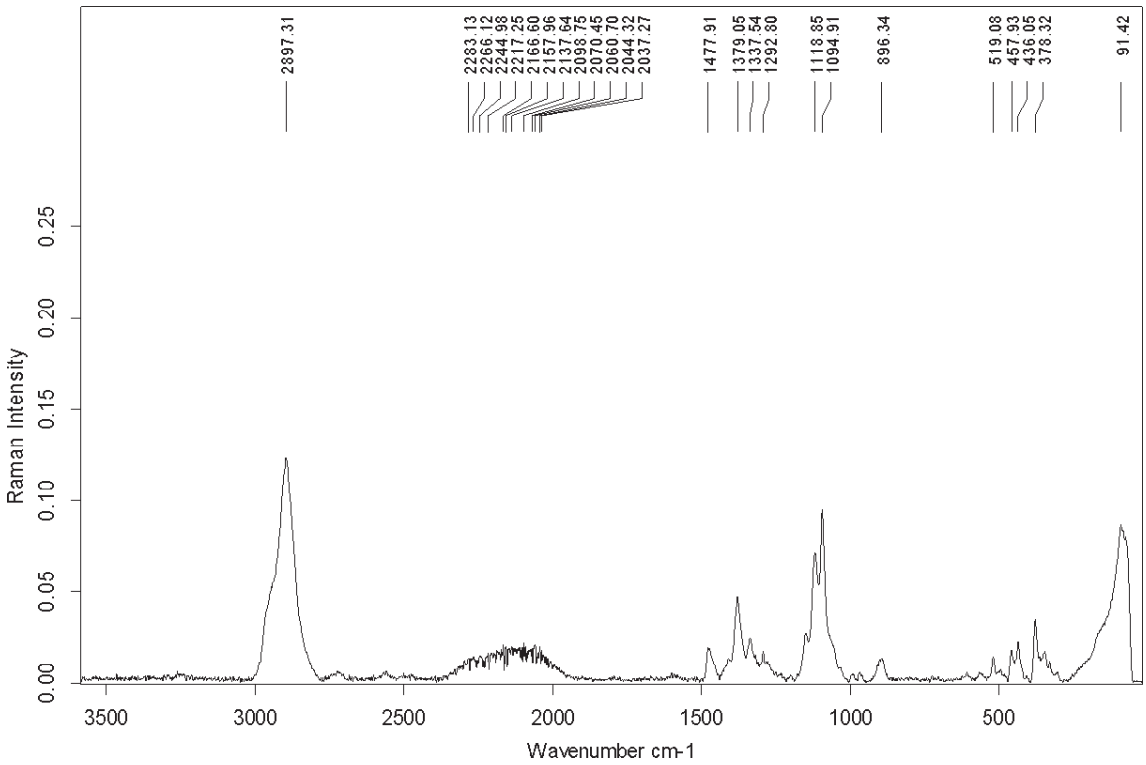

Figure 5.—Fourier-transform–Raman spectra of the nanocrystalline cellulose.

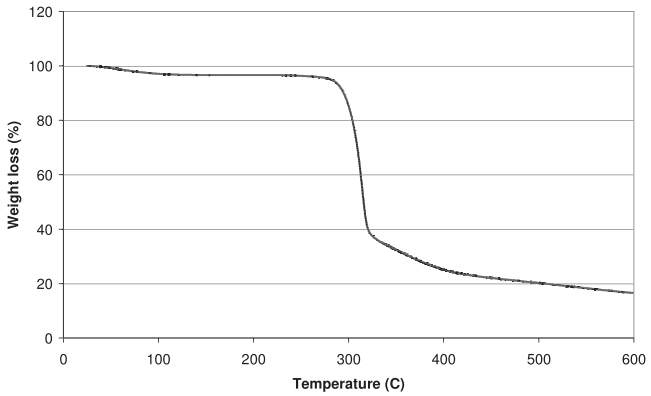

Figure 6.—Weight loss of the nanocrystalline cellulose during thermogravimetric analysis.

eau 1971). The first is the depolymerization reaction, and the second is the decomposition of the cellulose, which in several exothermic reactions produced gaseous products and residual char.

Refractive index

Determination of the RI of solid materials (e.g., powders) is quite complex. The well-known method for the determination of the RI of particles is the Becke Line microscopy method. In this method, particles are dispersed in liquids in which they do not dissolve. However, this method only works for the particles larger than 50 μm. For smaller particles, other methods need to be explored and developed. For example, if possible, the semitransparent, thin films made of small particles (e.g., nano size) might be used with an ellipsometer to determine of the RI of these particles. In the present study, a method developed by Saveyn et al. (2002) was adopted. In this method, the bulk RI of water-dispersible particles can be measured by determining the RI index of solutions formed by dissolving or dispersing the particles in an appropriate solvent. The RI recorded for known solute concentrations can be linearly extrapolated to 100 percent concentration to calculate the bulk RI. Figure 7 shows the RI of different solutions, DI water, DMSO-based solvent (Köhler and Heinze 2007), and MMNO versus the NCC concentration ranging from 0.2 to 1 percent by weight.

The graphs in Figure 7 revealed that the relationship between the RI of the NCC solutions and the NCC concentration is linear. The bulk RI of the NCC in each solution was calculated using the equation of the best-fit line. Table 1 presents the results obtained for each solution. The average obtained from three NCC solutions was 1.499. This result was validated using an ellipsometer to measure the RI of semitransparent, thin NCC films. The value obtained by the ellipsometer was approximately 1.5. Both results are in agreement. Compared with several reinforcing agents, such as silica, aluminum oxide, and titanium oxide, the NCC has a low RI. For this reason, it is possible to add the NCC in various plastics and coatings and retain good transparency.

Hardness

Figure 8 shows the curve of load versus depth under different force values. The graph confirms that the tests are reliable and repeatable for different applied forces.

Figure 9 shows how hardness and reduced Young's modulus of the NCC films were calculated. The hardness and Young's modulus of the NCC were 0.26 and 6.5 GPa, respectively. The measured values for the NCC are

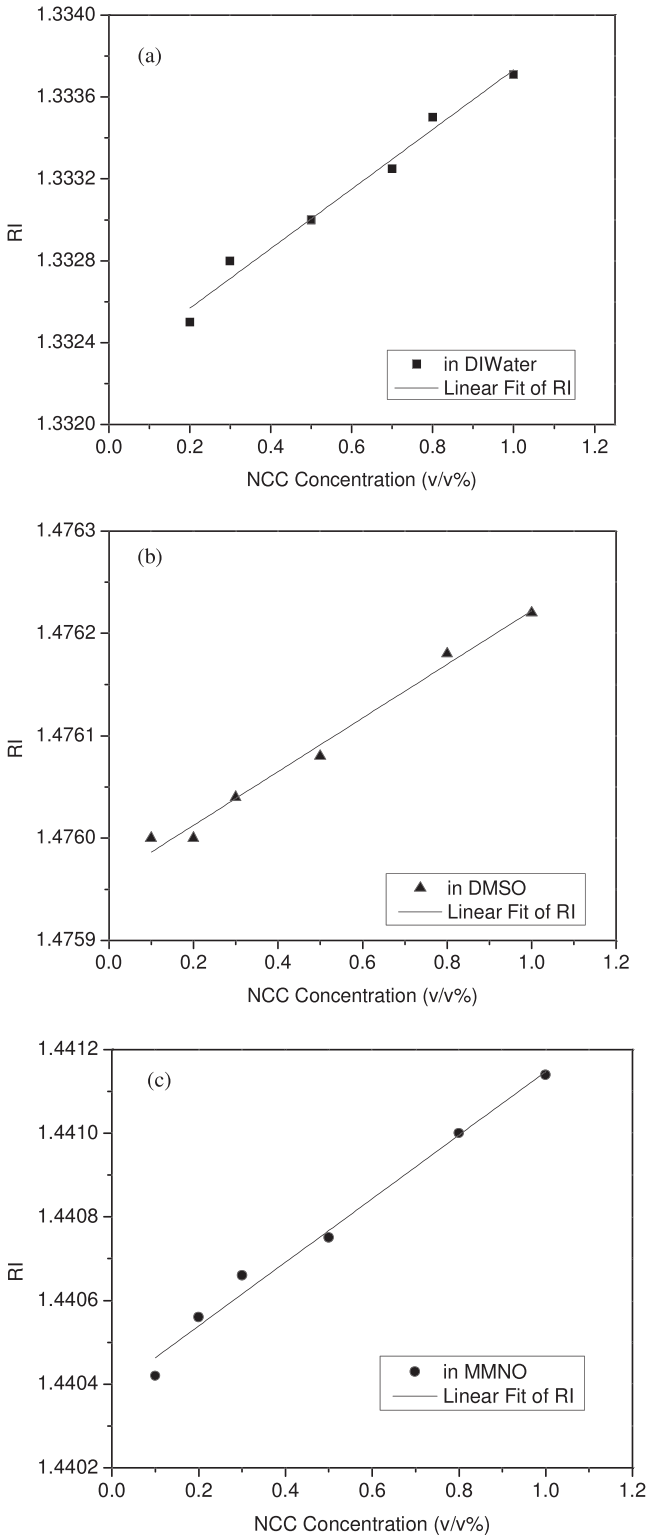

Figure 7.—Refractive index of the nanocrystalline cellulose in (a) distilled (DI) water, (b) dimethyl sulfoxide (DMSO)–based solvent, and (c) 4-methylmorpholine N*-oxide (MMNO).*

comparable to those of other cellulose fibrils studied in the literature. For example, Zimmermann et al. (2006) measured the modulus of the cellulose nanofibrils obtained from sulfite pulp and found it to be 6 GPa. In their work, the cellulose nanofibrils were used to reinforce hydroxypropyl-

Table 1.—The refractive index (RI) and mechanical properties of the nanocrystalline cellulose (NCC).[a]

Solvent used	RI of bulk NCC	Hardness (GPa)	Young's modulus (GPa)
DI water	1.4783		
DMSO	1.502		
MMNO	1.516		
No solvent		0.26	6.5
Average	1.499		
SD	0.0193		

[a] DI = distilled; DMSO = dimethyl sulfoxide; MMNO = 4-methylmorpholine *N*-oxide.

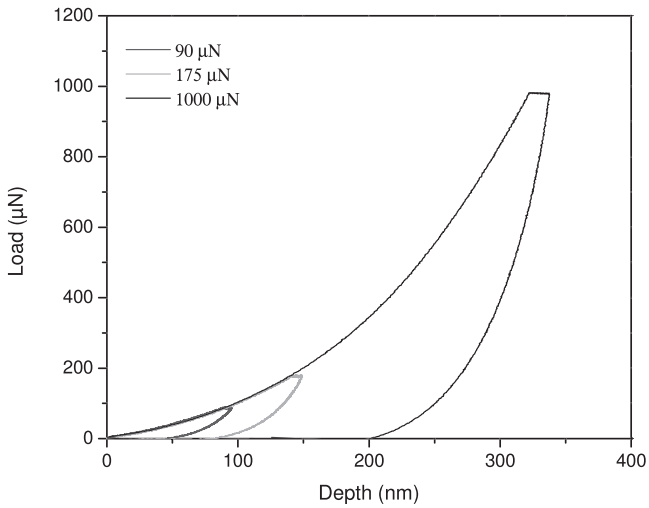

Figure 8.—Load-displacement curves.

cellulose polymer, which has a much lower modulus (1.3 GPa). This value was doubled with the addition of 10 percent (wt/wt) of the cellulose nanofibrils. Here, the results show that the addition of the NCC with high hardness value and Young's modulus into polymers should improve the mechanical performance of the resultant nanocomposite products.

Oil absorption

To determine the oil absorption as well as the moisture content of the NCC particles, three different particle sizes were prepared. Figure 10 presents the NCC particles prepared with the jar mill treatment (Fig. 10a) and the laboratory mill treatment (aperture, 0.5 mm; Fig. 10b). The particles prepared with the laboratory mill for the 0.5- and 1.0-mm apertures were 375 and 750 μm, respectively.

Oil absorption experiments were performed on the three powders prepared from the freeze-dried NCC. Oil absorption values are strongly affected by the particle size, surface area, and surface chemistry of the particles. Oil absorption represents the minimum weight of oil required to coat each pigment particle and to fill the voids between them (Morgans 1969). It is therefore a value that can be used to perform the quality control for different batches of particles. Moreover, this value is important for those formulating coatings or inks, because it gives a good indication of the amount of resin that can be absorbed by the particles rather than the amount available for film formation. Table 2

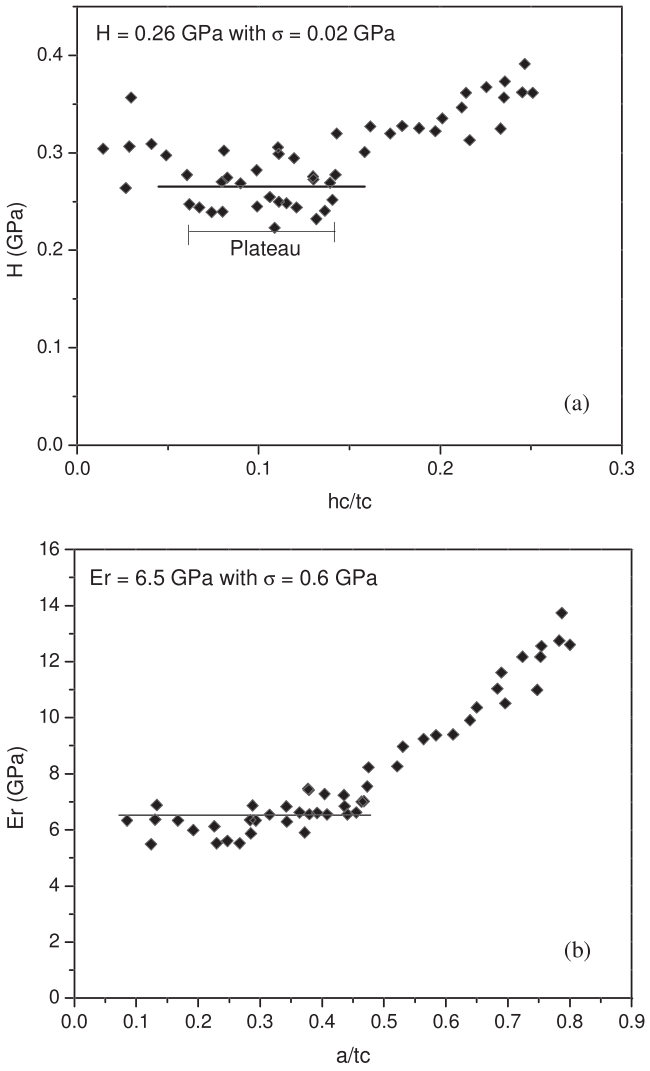

Figure 9.—(a) Hardness and (b) reduced Young's modulus of the nanocrystalline cellulose as a function of hc/tc *and* a/tc, *respectively.*

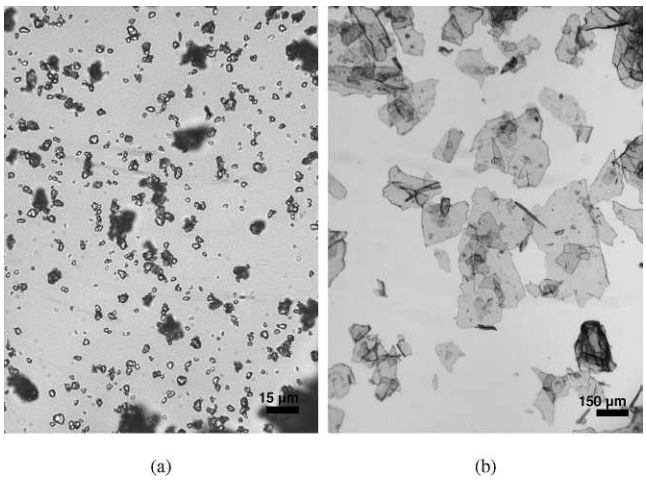

Figure 10.—(a) Particles obtained after the jar mill treatement (original magnfiication ×400) and (b) particles obtained following the treatment with the laboratory mill (aperture, 0.5 mm; original magnification ×40).

Table 2.—Oil absorption values for the three powders.

Particle size (µm)	Oil absorption (g/100 g)
4	72
375	399
750	856

presents the results of the oil absorption experiments for 100 g of particle for the three different powders used in the present study. As can be seen, the oil absorption increases with the particle size, which means that the bigger the NCC aggregates, the greater the absorption. These values are quite important if we compare them with those of china clay (30 g/100 g) and the amorphous silica (20 g/100 g) with a mean particle size of approximately 10 µm. These tests should be done by the same operator to ensure that comparative results are obtained.

Moisture content

Moisture content of each powder was determined following 48 hours in an oven at 105°C. Results are presented in Table 3 and reveal that the larger the particle size, the lower the moisture content after 48 hours in an oven. As can be seen, the moisture contents obtained are quite high, which can lead to problems in dispersing nanocrystals in polymer matrices. It also means that it is important to dry NCC powders carefully to be sure that they will not cause dispersion problems in hydrophobic polymers.

Conclusions

Nanocrystalline cellulose presents interesting results and could be used as a reinforcing agent in the plastics and coatings industries. The results from this study show that the NCC produced from the acid hydrolysis of pulp has high crystallinity (XRD, 78%; FT-Raman, 74%), hardness, and reduced Young's modulus. High crystallinity means better chemical resistance, which is important in the paint, plastics, and coatings industries. With its high Young's modulus, it is an important candidate reinforcing fiber in many polymer-based composites. The RI of the NCC was also measured and found to be lower than those of many reinforcing agents used in the plastics and coatings industries. This means that use of the NCC should not impact the transparency of the polymers. The NCC was also found to have high thermal stability. The degradation starts at approximately 290°C, which allows the NCC to be processed safely in many plastics. Oil absorption and moisture content were also measured for particles of different size. These experiments show that the oil absorption of the NCC increases with the particle size. Oil absorption needs to be kept as low as possible; therefore, it is preferable to work with low particle size. Small particles usually have a higher moisture content after drying, and it is therefore important to dry the smaller particles carefully before their addition in hydrophobic materials.

Table 3.—Moisture content of the three powders.

Particle size (µm)	Moisture content (%)
4	14.4
375	5.5
750	6.4

Literature Cited

Agarwal, U. P., R. S. Reiner, and S. A. Ralph. 2009. Determination of cellulose I crystallinity by FT-Raman spectroscopy. Paper No. P-053_ISWFPC_Celulose_Crystallinity. *In:* Proceedings of the 15th International Symposium on Wood, Fiber and Pulping Chemistry, June 15–18, 2009, Olso, Norway; Congress-Conference AS, Oslo Norway. http://www.treesearch.fs.fed.us/pubs/33710. Accessed June 20, 2011.

Agarwal, U. P., R. S. Reiner, and S. A. Ralph. 2010. Cellulose I crystallinity determination using FT-Raman spectroscopy: Univariate and multivariate methods. *Cellulose* 17:721–723.

Alemdar, A. and M. Sain. 2008. Isolation and characterization of nanofibers from agricultural residues—Wheat straw and soy hulls. *Bioresour. Technol*. 99(6):1664–1671.

American Society for Testing and Materials (ASTM). 1995. Standard method for oil absorption of pigments by spatula rub-out. ASTM D281-95. ASTM, Philadelphia.

Arseneau, D. F. 1971. Competitive reactions in the thermal decomposition of cellulose. *Can. J. Chem*. 49(4):632–638.

Beck-Candanedo, S., M. Roman, and D. G. Gray. 2005. Effect of reaction conditions on the properties and behavior of wood cellulose nanocrystal suspensions. *Biomacromolecules* 6(2):1048–1054.

Bhatnagar, A. and M. Sain. 2005. Processing of cellulose nanofiber-reinforced composites. *J. Reinf. Plast. Compos*. 24:1259–1268.

Borysiak, S. and B. Doczekalska. 2005. X-ray diffraction study of pine wood treated with NaOH. *Fibres Textiles East. Eur*. 13(5):87–89.

Cao, X., H. Dong, and C. M. Li. 2007. New nanocomposite materials reinforced with flax cellulose nanocrystals in waterborne polyurethane biomacromolecules. *Biomacromolecules* 8(3):899–904.

Chen, H.-L. and A. Yokochi. 2000. X-ray diffractometric study of microcrystallite size of naturally colored cottons. *J. Appl. Polym. Sci*. 76:1466–1471.

Clowes, F. A. L. and B. E. Juniper. 1968. Plant Cells. Blackwell Scientific, Edinburgh. 546 pp.

Côté, W. A. 1964. Cellular Ultrastructure of Woody Plants. Syracuse University Press, Syracuse, New York. pp. 1–31, 191–198.

Deepa, B., E. Abraham, B. M. Cherian, A. Bismark, J. J. Blaker, L. A. Pothan, A. L. Leao, S. F de Souza, and M. Kottaisamy. 2010. Structure, morphology and thermal characteristics of banana nano fibers obtained by steam explosion. *Bioresour. Technol*. 102: 1988–1997.

Dong, M. X., J. F. Revol, and D. G. Gray. 1998. Effect of microcrystallite preparation conditions on the formation of colloid crystals of cellulose. *Cellulose* 5(1):19–32.

Dufresne, A., J. Caville, and M. Vignon. 1997. Mechanical behavior of sheets prepared from sugar beet cellulose microfibrils. *J. Appl. Polym. Sci*. 64(6):1185–1194.

Dufresne, A. and M. Vignon. 1998. Improvement of starch film performances using cellulose microfibrils. *Macromolecules* 31(8): 2693–2696.

Favier, V., G. Canova, J. Y. Cavaille, H. Chanzy, A. Dufresne, and C. Gauthier. 1995a. Nanocomposite materials from latex and cellulose whiskers. *Polym. Adv. Technol*. 6(5):351–355.

Favier, V., H. Chanzy, and J. Y. Cavaille. 1995b. Polymer nanocomposites reinforced by cellulose whiskers. *Macromolecules* 28: 6365–6367.

Fengel, D. and G. Wegener. 1984. Wood: Chemistry, Ultrastructure, Reactions. Walter de Gruyter & Co., Berlin. 613 pp.

Fink, H. P., B. Philipp, B. Paul, R. Serimaa, and T. Paakkari. 1987. The structure or amorphous cellulose as revealed by wide-angle x-ray scattering. *Polymer* 28(8):1265–1270.

Grunert, M. and W. T. Winter. 2002. Nanocomposites of cellulose acetate butyrate reinforced with cellulose nanocrystals. *J. Polym. Environ*. 10(1/2):27–30.

Hamad, W. Y. and T. Q. Hu. 2010. Strcuture-process-yield interrelations in nanocrystalline cellulose extraction. *Can. J. Chem. Eng*. 88: 392–402.

Köhler, S. and T. Heinze. 2007. New solvents for cellulose: Dimethyl sulfoxide/ammonium fluorides. *Macromol. Biosci*. 7(3):307–314.

Morgans, Q. M. 1969. Outlines on Paint Technology. Charles Griffin and Company Ltd., London. 224 pp.

Nakagaito, A. N. and H. Yano. 2004. The effect of fiber content on the mechanical and thermal expansion properties of biocomposites based on microfibrillated cellulose. *Appl. Phys. A Mater. Sci. Process*. 76: 2080–2092.

Nishiyama, Y., P. Langan, and H. Chanzy. 2002. Crystal structure and hydrogen-bonding system in cellulose 1β from synchrotron x-ray and neutron fiber diffraction. *J. Am. Chem. Soc*. 124(31):9074–9082.

Oh, S. Y., D. I. Yoo, Y. Shin, H. C. Kim, H. Y. Kim, Y. S. Chung, W. H. Park, and J. H. Youk. 2005. Crystalline structure analysis of cellulose treated with sodium hydroxide and carbon dioxide by means of x-ray diffraction and FTIR spectroscopy. *Carbohydr. Res*. 340:2376–2391.

Ohad, I. and C. Mejzler. 1965. On the ultrastructure of cellulose microfibrils. *J. Polym. Sci. Part A-1 Polym. Chem*. 3(1):399–406.

Proniewicz, L. M., C. Paluszkiewicz, A. Weselucha-Birczynska, H. Majcherczyk, A. Baranski, and A. Konieczna. 2001. FT-IR and FT-Raman study of hydrothermally degradated cellulose. *J. Mol. Struct*. 596(1):163–169.

Randriamanantena, T., F. L. Razafindramisa, G. Ramanantsizehena, A. Bernes, and C. Lacabane. 2009. Thermal behaviour of three woods of Madagascar by thermogravimetric analysis in inert atmosphere. *In:* Proceedings of the Fourth High-Energy Physics International Conference, August 21–28, 2009, Antananarivo, Madagascar. http://www.slac.stanford.edu/econf/C0908211/proceedings.htm. Accessed June 20, 2011.

Rosa, M. F., E. S. Medeiros, J. A. Malmonge, K. S. Gregorski, D. F. Wood, L. H. C. Mattoso, G. Glenn, W. J. Orts, and S. H. Iman. 2010. Cellulose nanowhiskers from coconut husk fibers: Effect of preparation conditions on their thermal and morphological behavior. *Carbohydr. Polym*. 81(1):83–92.

Rydholm, S. A. 1965. Pulping Processes. Interscience Publishers, New York. pp. 90–156.

Saveyn, H., D. Mermuys, O. Thas, and P. van der Meeren. 2002. Determination of the refractive index of water-dispersible granules for use in laser diffraction experiments. *Part. Part. Syst. Charact*. 19(6): 426–432.

Schenzel, K., H. Almlöf, and U. Germgård. 2008. A new method determining quantitatively the polymorphic transformation, cellulose I → cellulose II, by utilizing FT Raman data of cellulose pulps. *In:* Proceedings of the XXIth International Conference on Raman Spectroscopy, August 17–22, 2008, West London; IM Publications, Chichester, West Sussex, UK. p. 797.

Wang, H.-Y. and M.-F. Huang. 2007. Preparation, characterization and performances of biodegradable thermoplastic starch. *Polym. Adv. Technol*. 18(11):910–915.

Wiley, J. H. and R. J. Atalla. 1987. Band assignments in the Raman spectra of celluloses. *Carbohydr. Res*. 160:113–129.

Zimmermann, T., E. Pohler, T. Geiger, J. Schleuniger, P. Schwaller, and K. Richter. 2006. Cellulose fibrils: Isolation, characterization, and capability for technical applications. *In:* Cellulose Nanocomposites: Processing, Characterization, and Properties. K. Oksman and M. Sain (Eds.). ACS Symposium Series 938. American Chemical Society, Washington, D.C.